Eklund, Kim; Kuklin, Mikhail S.; Kraus, Florian; Karttunen, Antti J.

Evolutionary Algorithm-based Crystal Structure Prediction for Gold(I) Fluoride

Published in:
ChemPhysChem

DOI:
10.1002/cphc.201901070

Published: 20/04/2020

Document Version
Peer-reviewed accepted author manuscript, also known as Final accepted manuscript or Post-print

Evolutionary Algorithm-based Crystal Structure Prediction for Gold(I) Fluoride

Kim Eklund, Mikhail S. Kuklin, and Antti J. Karttunen*
Department of Chemistry and Materials Science,
Aalto University, P.O. Box 16100, FI-00076 Aalto, Finland

Florian Kraus
Fachbereich Chemie, Philipps-Universität Marburg,
Hans-Meerwein-Strasse 4, 35032, Marburg, Germany
(Dated: January 2, 2020)

Solid gold(I) fluoride remains as an unsynthesized and uncharacterized compound. We have performed a search for potential gold(I) fluoride crystal structures using USPEX evolutionary algorithm and dispersion-corrected hybrid density functional methods. Over 4000 AuF crystal structures have been investigated. Behavior of the AuF crystal structures under pressure was studied up to 25 GPa, and we also evaluated the thermodynamic stability of the hypothetical AuF crystal structures with respect to AuF_3, AuF_5, and Au_3F_8. Mixed-valence crystal structure $Au_3[AuF_4]$ with Au atoms in various formal oxidation states emerged as the thermodynamically most stable AuF species.
Keywords: Gold, Fluorides, Aurophilicity, Structure elucidation, Density functional calculations

I. INTRODUCTION

Along with copper(I) fluoride, gold(I) fluoride remains as a so far inconclusively synthesized and characterized group 11 binary monohalide [1, 2]. The other gold(I) monohalides, gold(I) chloride, gold(I) bromide, and gold(I) iodide, are known, all having tetragonal crystal structures consisting of polymer-like zig-zag links of alternating Au and halogen atoms [3–5]. AuCl ($I4_1/amd$) and AuBr ($I4_1/amd$ and $P4_2/ncm$) can be prepared by controlled thermal decomposition of $AuCl_3$ and $AuBr_3$, respectively. AuI ($P4_2/ncm$) has been prepared by reacting a gold(III) salt with potassium iodide and by a direct reaction of gold metal and iodine [1].

Three binary gold fluorides are known: gold(III) fluoride AuF_3, gold(V) fluoride AuF_5, and gold(II,III) fluoride Au_3F_8. AuF_3 can be prepared for example either by reacting gold metal with BrF_3 and removing the remaining BrF_3 by heating, or by direct low-pressure, high-temperature fluorination of gold metal [6, 7]. The crystal structure consists of corner-sharing square-planar AuF_4 units forming one-dimensional infinite chains [8]. AuF_5 can be prepared by oxidising gold metal with krypton difluoride or by heating gold in the presence of oxygen and fluorine [9, 10]. In both cases, an intermediate salt containing $[AuF_6]^-$ anions decomposes to AuF_5. The structure is dimeric, Au_2F_{10}, unlike that of any other known pentafluoride such as MoF_5 [11, 12]. The crystal structure of AuF_5 is isotypic with $\gamma-MoCl_5$ [13] and $NbBr_5$ [14]. Mixed-valent Au_3F_8, which can be described as $Au(II)[Au(III)F_4]_2$, has been reported to be a simple paramagnet [15, 16].

A synthesis of gas-phase gold(VII) fluoride, AuF_7, from the reaction of AuF_5 and atomic fluorine has also been reported [17], but later computational studies suggest that the reported compound is in fact the complex $AuF_5 \cdot F_2$ [18, 19]. Contemporary attempts to replicate the synthesis route have only yielded AuF_5 [20].

Previously, it was thought that the preparation of gold(I) fluoride would simply be impossible based on thermodynamic estimates of Waddington [21]. Later quantum chemical studies suggested that AuF could actually exist both in the gas phase and the solid state [22–24]. Since then, molecular AuF has been characterized in the gas phase by neutralization-reionization mass spectroscopy [25], emission spectroscopy [26], and microwave spectroscopy [27]. In addition, Ne–AuF and Ar–AuF species have been observed in noble gas matrices using matrix infrared spectroscopy [28].

The first computational studies on possible AuF solid state structures by Schwerdtfeger *et al.* [29, 30] focused on structure types known for binary group 11 halides such as the zinc blende ($F\bar{4}3m$) and rock salt ($Fm\bar{3}m$) structure types, as well as the chain-like tetragonal gold halide structures discussed above. Grochala and Kurzydłowski [31] studied potential AuF solid state structures by starting from the rock salt, CsCl ($Pm\bar{3}m$), AuCl, and AuI structures. They found that these structures were not true local minima for AuF. The structures were then distorted in the direction of imaginary phonon modes and re-optimized. At 5 GPa, a new orthorhombic $Cmcm$ modification was found to have the lowest energy (Figure 1). A transition to a high-pressure tetragonal phase ($P4/nmm$) at 20 GPa was also predicted (Figure 1). High pressure comproportionation $AuF_3 + 2\ Au \rightarrow 3\ AuF$ was proposed as a synthesis route. They also investigated the use of xenon as a mediator to obtain AuF at lower pressures [32].

Nowadays, a multitude of approaches are available for predicting novel crystal structures with quantum chemical methods [33, 34]. Evolutionary algorithms mimicking evolutionary principles provide a way to explore a much larger search space than predictions based on known structure types. The use of structure prediction algorithms enables the evaluation of potential structures

* antti.j.karttunen@iki.fi

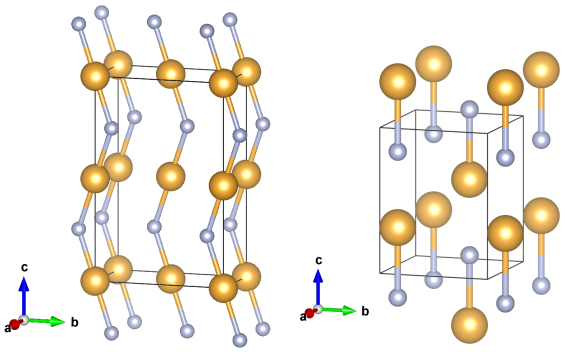

Figure 1. AuF crystal structures predicted by distorting known binary group 11 halide structures [31]. Left: *Cmcm* structure (**C**), right: $P4/nmm$ structure (**H**).

which may adopt an unexpected or unique structure type [35–37]. Evolutionary algorithms have so far been used successfully in many structural prediction studies of transition metal compounds and prospective materials based on them, both at ambient and higher pressures [38–42]. The valence states of gold in Au–F compounds under high pressure have very recently been studied by Liu *et al.* using particle swarm optimization and density functional theory (DFT) [43]. They predicted two new AuF crystal structures (Figure 2).

We describe an evolutionary algorithm -based crystal structure prediction study for gold(I) fluoride using the USPEX (Universal Structure Predictor: Evolutionary Xtallography) algorithm and dispersion-corrected hybrid density functional methods. We have recently used the same methodology for investigating copper(I) fluoride, resulting in several novel structural candidates that possess lower energy than the previously reported hypothetical CuF crystal structures [42]. We also investigate the known binary gold fluorides AuF_3, AuF_5, and Au_3F_8 and the previously reported hypothetical AuF crystal structures at the same level of theory.

II. COMPUTATIONAL DETAILS

Version 9.4.4 of the USPEX code was used for the crystal structure predictions [44–46]. Quantum chemical calculations within the USPEX simulations were carried out with the CRYSTAL [47] code using the USPEX interface we have developed [41]. In the DFT calculations, we applied a hybrid PBE0 functional with 25% Hartree-Fock exchange [48, 49]. The aurophilic $d^{10} \cdots d^{10}$ interaction of Au(I) [50–52] was included in the USPEX search by using Grimme's D3 dispersion correction with zero-damping (ZD) [53, 54]. The hybrid DFT-PBE0 functional has been shown to produce consistent structures and energetics for a number of *d*-metal fluorides.[55, 56]

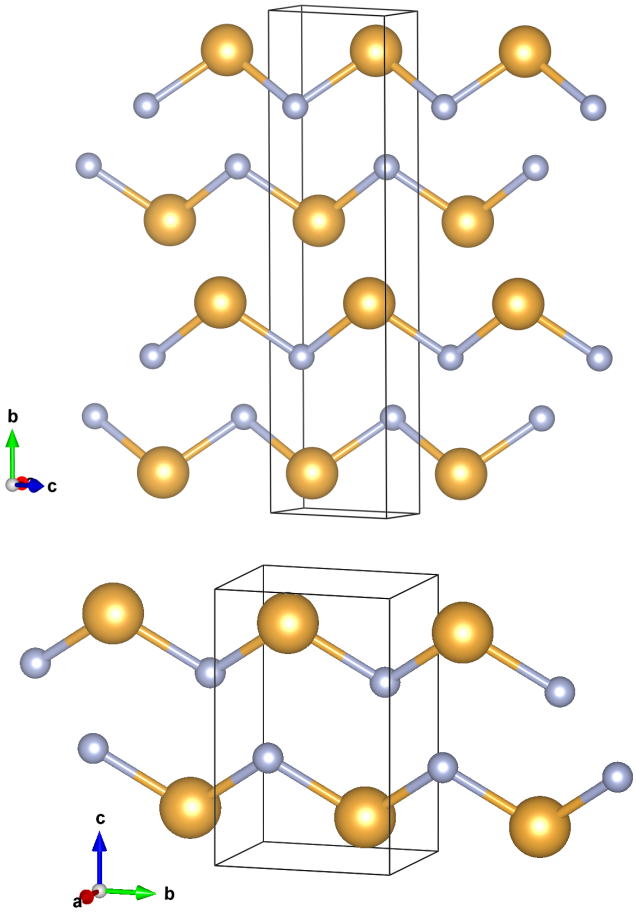

Figure 2. AuF crystal structures predicted with particle swarm optimization algorithm [43]. Top: $P2_1/c$ (corresponding to **D**), bottom: $P2_1/m$ structure (**E**).

We have recently used the DFT-PBE0-D3 approach to investigate hypothetical copper(I) fluorides and in addition to describing the cuprophilic $d^{10} \cdots d^{10}$ interactions, the method also properly described the experimentally known group 11 fluorides CuF_2 and AgF.[42] The basis sets used were Gaussian-type triple-ζ-valence + polarization (TZVP) and split-valence + polarization (SVP) derived from molecular Karlsruhe def2 basis sets [57].

In the USPEX simulations, we used different numbers of formula units (Z) to study the configuration space of the unknown crystal structure of AuF. Formula units were investigated from $Z = 2$ to $Z = 8$, and except for the computationally more demanding $Z = 7$ and $Z = 8$, two USPEX simulations were carried out. Composition $Z = 1$ was judged to be too small already in our previous study for CuF [42]. Composition $Z = 4$ was found to produce the lowest energy structure, and thus two further USPEX simulations were carried out with $Z = 4$ using an external hydrostatic pressure of 20 GPa in the CRYSTAL geometry optimizations. To speed up the evolutionary searches, the CRYSTAL geometry optimizations within the USPEX simulations were carried out with looser con-

vergence criteria compared to the criteria reported below. Three structural optimizations with increasingly strict convergence criteria were carried out for each structural candidate. Reciprocal space k-point density of 0.10, 0.08, and 0.06 2πÅ^{-1} was applied for the first, second, and third optimization steps, respectively. For the compositions from $Z = 2$ to $Z = 6$, we used two different basis set combinations in the USPEX simulations: (1) SVP in all three optimization steps and (2) TZVP in the third optimization step. Similar results were obtained from both approaches. Input examples for USPEX and CRYSTAL are included in the Supporting Information.

The lowest-energy structures from each USPEX simulation were re-optimised at the DFT-PBE0-D3(ZD)/TZVP level of theory and the default CRYSTAL convergence criteria. Reciprocal space k-point meshes were chosen in such way that the reported energies are converged to about 0.1 kJ/mol per atom. The used k-point meshes are reported in the Supporting Information. Using Fermi smearing (0.001 a.u.) or double-density k-meshes for the evaluation of the Fermi energy did not have any significant effect on the energetics or geometries of conducting AuF crystal structures. The band gaps reported for the semiconducting structures in Tables I and II were obtained directly from the SCF calculations and confirmed by using double-density k-meshes. Tightened tolerance factors (TOLINTEG) of 8, 8, 8, 8 and 16 were used for the evaluation of the Coulomb and exchange integrals. The same computational settings were used to study the previously reported hypothetical AuF crystal structures [31, 43].

All low-energy AuF structures discussed here were confirmed as true local minima by means of a harmonic frequency calculation [58, 59]. To study the thermodynamics of the comproportionation reaction AuF_3 + 2 Au $\rightarrow$ 3 AuF and the formation enthalpies of binary gold fluorides, we also investigated F_2, Au, AuF_3, AuF_5, and Au_3F_8 at the same DFT-PBE0-D3(ZD)/TZVP level of theory (see Supporting Information for full computational details on the experimentally known reference species). All thermodynamic properties were evaluated within the harmonic approximation.

To benchmark the applied DFT-PBE0-D3(ZD)/TZVP level of theory, we carried out a full structural optimization of experimentally known AuCl ($I4_1/amd$) discussed in the Introduction. The Au–Cl bond lengths and the aurophilic Au(I)...Au(I) distances are reproduced well in comparison to experiment: The optimized Au–Cl distance of 2.37 Å is elongated by 3.0% in comparison to experiment (2.37 Å vs. 2.30 Å), while the shortest Au(I)$\cdots$Au(I) distance is 0.8% longer in the case of the optimized structure (3.25 Å vs. 3.23 Å). The optimized structure of AuCl is included as supporting information.

Table I. Relative energies, DFT-PBE0 and DFT-HSE06 band gaps, and densities of the lowest-energy AuF crystal structures **A**–**E** at 0 GPa. Z is the number of formula units.

Struct.	Space group (no.)	Z	ΔE (kJ/mol)	PBE0 gap (eV)	HSE06 gap (ev)	Density (g/cm^3)
A	$P\bar{1}$ (2)	4	0.0	no gap	no gap	12.56
C	$Cmcm$ (63)	2	14.0	1.1	0.4	11.81
B	$P3_1$ (144)	3	15.3	1.0	0.4	11.84
D	$Pnma$ (62)	4	18.7	no gap	no gap	12.71
E	$P2_1/m$ (11)	2	18.7	no gap	no gap	12.80

III. RESULTS

A. Overview of the lowest-energy AuF crystal structures predicted with USPEX

Summary of the predicted lowest-energy AuF crystal structures is presented in Table I. The lowest-energy crystal structure **A** found in our search is used as reference in energy comparisons. All relative energies of the AuF crystal structures are reported with respect to **A**:

$$\Delta E = E(\text{structure})/Z(\text{structure}) - E(\mathbf{A})/Z(\mathbf{A}) \quad (1)$$

From composition $Z = 3$ upwards, the lowest-energy crystal structures predicted with USPEX were in fact no longer gold(I) fluorides, but contained gold atoms in various formal oxidation states. The lowest-energy crystal structure from our USPEX simulations (**A**) was obtained with $Z = 4$ (Figure 3). It was obtained from USPEX simulations with $Z = 4$ both at 0 and 20 GPa. The structure **A** adopts a triclinic crystal structure ($P\bar{1}$) containing layers of square-planar AuF_4 units sandwiched between layers of gold atoms. Within the square-planar units the Au–F distances are 1.97 Å. This Au–F distance is in good agreement with experimentally determined Au–F distances in MAuF$_4$ (M = Li–Cs) [60–62]. Each AuF_4 unit is connected to two Au atoms *via* bridging F atoms with a rather long F–Au distance of 2.28 Å. The gold layer itself can be viewed as a structure of three layers of gold atoms. The gold atoms in the central layer are 8-coordinated, forming a square prism reminescent of a body centered cubic (bcc) arrangement. The Au atoms in the prism vertices are each connected to one F atom of the AuF_4 units. The Au–Au distance of 2.67 Å between the vertex atoms is rather short, corresponding to the prism height. The Au–Au distances between the central Au atom and the prism vertices are between 2.84 – 2.88 Å, which is very similar to distances in bulk gold (2.88 Å) [63]. The mixed-valence crystal structure **A** can also be described with the structural formula $Au_3[AuF_4]$.

The metallic gold layers in the crystal structure **A** are reminescent of the metallic sublattice in silver subfluoride Ag_2F.[64] Ag_2F crystallizes in the anti-CdI_2 structure type and is a metal, similar to the mixed-valence crystal structure $Au_3[AuF_4]$ (**A**).[65, 66]

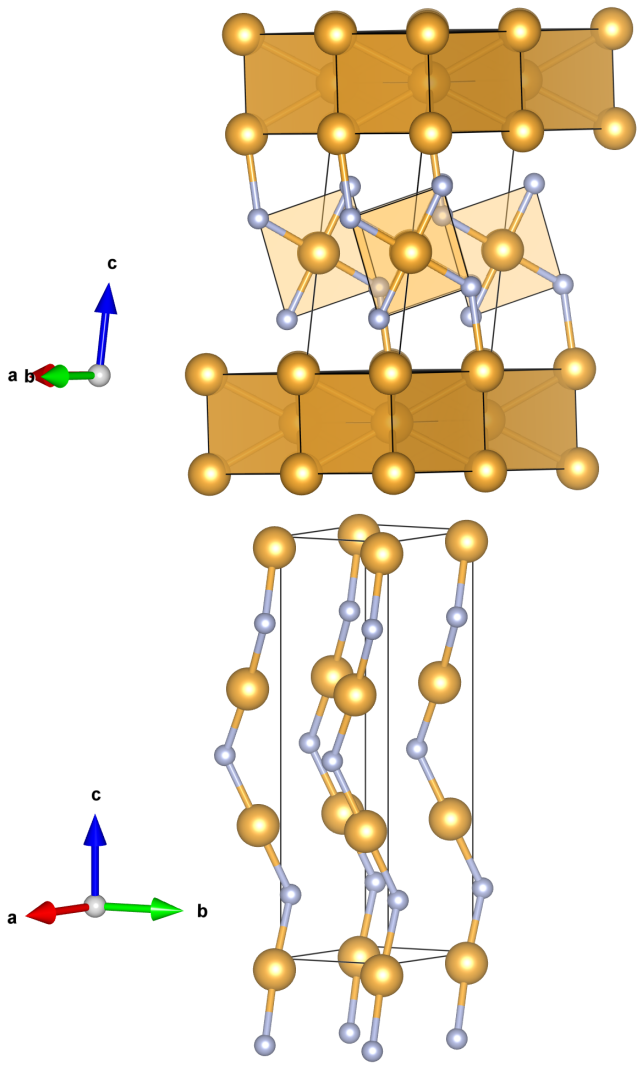

Figure 3. Crystal structure **A** ($P\bar{1}$, top) and **B** ($P3_1$, bottom). Gold atoms and their coordination polyhedra in yellow, fluorine atoms in blue.

To confirm the existence of a band gap in the crystal structures **B** and **C**, we calculated the band gap also with the screened Coulomb hybrid functional HSE06.[67] Crystal structures A, D, and E remain metallic, similar to the original PBE0 calculations. For the crystal structures B and C, the band gap is reduced from about 1.0 eV to 0.4 eV. This is in line with the fact that HSE06 should produce smaller band gaps in comparison to global hybrid PBE0.

Composition $Z = 3$ produced the highest-symmetry crystal structures of our USPEX simulations. They all adopt trigonal crystal structures reminiscent of the topology of the cinnabar structure type previously predicted for CuF [42, 68]. The lowest-energy $Z = 3$ structure **B** adopts the space group $P3_1$ (Figure 3). The Au–F distances within the chain are 2.10–2.11 Å and the inter-chain Au–Au distances are 3.03 Å. The other two trigonal crystal structures are isoenergetic and have enantiomorphic space groups $P3_121$ and $P3_221$.

With composition $Z = 2$, we obtained the previously predicted orthorhombic crystal structure **C** with space group $Cmcm$ (Figure 1) [31]. The Au–F distances within the chain are 2.10 Å and the inter-chain Au–Au distances are 2.98 Å.

Two high-pressure USPEX simulations with composition $Z = 4$ at 20 GPa also produced crystal structure **A** described above. Crystal structures analogous to the monoclinic structures predicted by Liu *et al.* were also reproduced by USPEX [43]. However, **D**, the analogue of the crystal structure in space group $P2_1/c$ (Figure 2) was obtained in the supergroup $Pnma$. When **D** is reoptimized at 0 GPa, the Au–F distances within the chain are 2.17 Å and the inter-chain Au–Au distances are 2.58 Å. For the crystal structure **E** ($P2_1/m$), the Au–F and Au–Au distances are identical to those in **D**.

In addition, several low-energy crystal structures with mixed-valence and chain-like features were found at 20 GPa (Fig 4). Their energetics are discussed in the next section. Crystal structure **F** ($Amm2$) with molecular AuF, AuF_2, and Au units building blocks was particularly interesting and was obtained in both 20 GPa USPEX simulations. Another crystal structure **G** ($C2$) containing mixed-valent Au atoms had even lower energy in comparison to **F** at 20 GPa. However, the symmetry of both structures lowered to $P1$ upon reoptimization at 0 GPa.

B. Effect of pressure on AuF structures

In order to understand the effect of pressure on the AuF structures obtained from our USPEX simulations, we also optimised the lowest-energy structures at an external hydrostatic pressure of 5 GPa, 10 GPa, 15 GPa, 20 GPa, and 25 GPa. Crystal structure **A** remained as the lowest-energy structure at all studied pressures. At 20 GPa, the coordination number of each gold atom in crystal structure **A** is higher compared to 0 GPa due to two new Au–Au contacts (2.83 Å). Relative energies of the AuF crystal structures in relation to the one of **A** at 20 GPa are presented in Table II. Here, we also include the previously reported tetragonal high-pressure crystal structure **H** ($P4/nmm$), which we did not obtain from our USPEX runs [31].

We also investigated the enthalpy of the comproportionation reaction $AuF_3 + 2\ Au \longrightarrow 3\ AuF$ at different pressures (Figure 5) similar to the approach of Kurzydłowski and Grochala.[31] Here, the reaction enthalpy $H_r = U + pV$ was evaluated by using the electronic energy E as U. Crystal structure **A** has the most favorable reaction enthalpy, even though at higher pressures crystal structures **D** and **E** become slightly more feasible. Similar to the previously reported hypothetical AuF crystal structures, even the most favorable crystal

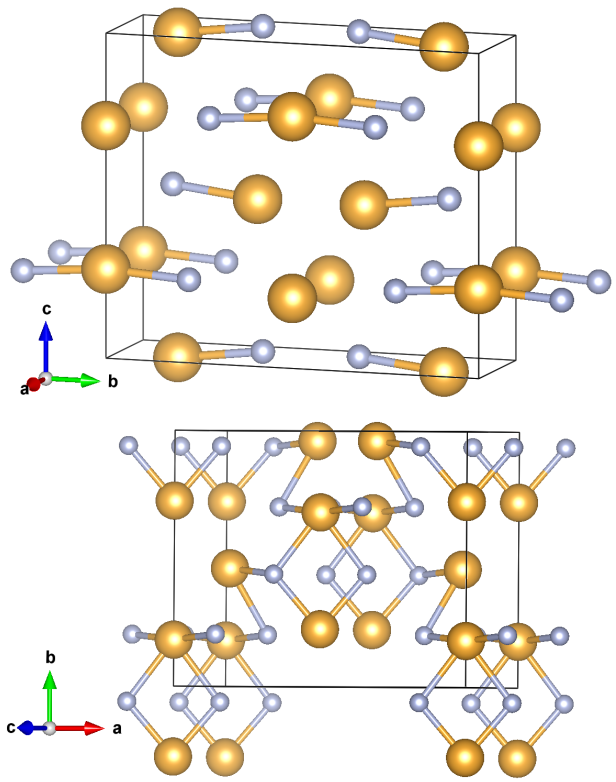

Figure 4. Crystal tructure **F** (*Amm*2, top) and **G** (*C*2, bottom) at 20 GPa. Gold atoms in yellow, fluorine atoms in blue.

Table II. Relative energies, band gaps, and densities of the lowest-energy AuF crystal structures **A**–**H** at 20 GPa. Z is the number of formula units.

Structure	Space group (no.)	Z	ΔE (kJ/mol)	Band gap (eV)	Density (g/cm^3)
A	$P\bar{1}$ (2)	4	0.0	no gap	14.76
G	$C2$ (5)	4	11.8	no gap	14.99
E	$P2_1/m$ (11)	4	12.9	no gap	14.97
D	*Pnma* (62)	4	13.1	0.1	14.94
F	*Amm*2 (38)	4	13.3	no gap	15.05
C	*Cmcm* (63)	2	27.6	0.8	14.27
H	$P4/nmm$ (129)	4	28.0	no gap	15.28
B	$P3_1$ (144)	3	28.1	0.7	14.32

structure **A** is only metastable with respect to decomposition to Au and AuF_3 at ambient pressure, but its stability should improve at elevated pressures.[31] At 25 GPa, crystal structure **B** becomes more favorable in comparison to the crystal structure **C**. Of interest here is the relation between crystal structures **C** and **H**. The use of hybrid DFT and the inclusion of dispersion correction in the quantum chemical calculations brings down the reported phase transition between these crystal structures from 20 GPa to 10 GPa [31].

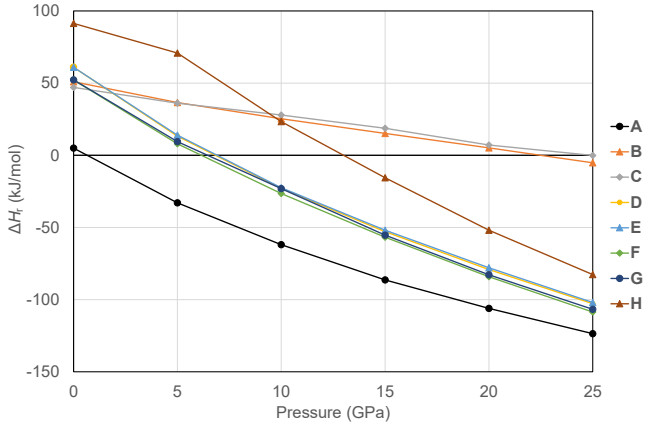

Figure 5. Reaction enthalpy ΔH_r of the comproportionation reaction $AuF_3 + 2\ Au \longrightarrow 3\ AuF$ for the reported AuF crystal structures **A**–**H**.

C. Enthalpies and Gibbs free energies of formation for binary gold fluorides

To study the thermodynamics of AuF in comparison to known binary gold fluorides AuF_3, AuF_5, and Au_3F_8, the standard enthalpies of formation and standard Gibbs free energies of formation for binary gold fluorides were calculated at 0 GPa in the temperature range 200–700 K. Harmonic frequencies were calculated for all structures to obtain the thermodynamic properties. Experimentally determined literature values for the standard enthalpy of formation of AuF_3 are –348.8 kJ/mol [69], –363.8 kJ/mol [70], and –413.2 kJ/mol [71]. For AuF_5, only the value –473.4 kJ/mol [71] has been reported and for Au_3F_8 no data has been reported. No experimental data on the standard Gibbs free energies of formation of binary gold fluorides was found. At 298.15 K, we obtained the values $\Delta_f H^\circ$ = –270 kJ/mol and $\Delta_f G^\circ$ = –199 kJ/mol for AuF_3, $\Delta_f H^\circ$ = –210 kJ/mol and $\Delta_f G^\circ$ = –92 kJ/mol for AuF_5, and $\Delta_f H^\circ$ = –788 kJ/mol and $\Delta_f G^\circ$ = –592 kJ/mol for Au_3F_8. For the hypothetical $Au_3[AuF_4]$ crystal structure **A**, the values $\Delta_f H^\circ$ = –91 kJ/mol $\Delta_f G^\circ$ = –65 kJ/mol were obtained.

The employed DFT-PBE0 method is known to overestimate the F–F bond strength and the F–F stretching frequency in F_2,[72] which may explain some of the differences between our calculated and the experimental enthalpies of formation for AuF_3 (–270 kJ/mol vs. –348.8 or –363.8 kJ/mol). The larger discrepancy between the calculated and experimentally obtained $\Delta_f H^\circ$ value for AuF_5 (–210 kJ/mol vs. –473.4 kJ/mol) might also partly be explained by the demanding experimental set-up which involved violent decomposition of AuF_5 in H_2O and NaOH. Likewise, the value for AuF_3 obtained in the same study [71] greatly differs from the values re-

Table III. Enthalpies (ΔH) and Gibbs free energies (ΔG) of reaction, according to eq. 2, at 300 K (normalized per atom). The experimental ΔH for AuF_3 has been reported as –87 or –91 kJ/mol per atom (see text).

Structure	ΔH (kJ/mol)	ΔG (kJ/mol)
Au_3F_8	–72	–54
AuF_3	–68	–50
$Au_3[AuF_4]$ (**A**)	–45	–32
AuF_5	–35	–15

ported in the two other references [69, 70].

To enable direct comparisons between binary gold fluorides with different compositions, the enthalpy of the formation reaction $x\mathrm{Au} + y\mathrm{F_2} \longrightarrow \mathrm{Au}_x\mathrm{F}_{2y}$ was normalized per atom and studied according to equation:

$$\Delta H = \{H(\mathrm{Au}_x\mathrm{F}_{2y}) - [xH(\mathrm{Au}) + yH(\mathrm{F_2})]\}/(x+2y) \quad (2)$$

The Gibbs free energy of formation reaction (ΔG) was calculated analogously.

ΔH and ΔG as a function of temperature are presented in Figure 6 and Figure 7, respectively. In addition, the values at 300 K are tabulated in Table III. The results clearly illustrate the metastability of AuF_5, with the value of ΔG becoming positive above 550 K. Au_3F_8 and AuF_3 remain as the thermodynamically most stable binary gold fluorides throughout the temperature range, even though at higher temperatures the gap in ΔG between them and the hypothetical AuF modifications is reduced. The lower value for ΔH of Au_3F_8 in comparison to AuF_3 is consistent with experimental observations on the formation of Au_3F_8 [15]. Bartlett *et al.* suggested that it is energetically more favorable to have Au(III) in an $[AuF_4]^-$ anion instead of neutral AuF_4 units in AuF_3, and therefore the solvolysis of $Au(SbF_6)_2$ by anhydrous HF produces $Au(II)[Au(III)F_4]_2$ instead of AuF_3. The energetical favorability of $[AuF_4]^-$ anions is also apparent from the $Au_3[AuF_4]$ crystal structure **A** found in our search.

IV. CONCLUSION

We have performed a systematic crystal structure prediction study for AuF with formula unit compositions from $Z = 2$ to $Z = 8$ using USPEX evolutionary algorithm and dispersion-corrected hybrid DFT method. Over 4000 crystal structures were investigated and structure prediction simulations were also carried out at a high pressure of 20 GPa. The energetics and thermodynamics of the lowest-energy crystal structures were studied in pressures up to 25 GPa and compared with experimentally known binary gold fluorides. The lowest-energy AuF crystal structure is not actually Au(I)F but a mixed-valence $Au_3[AuF_4]$ species, indicating that the

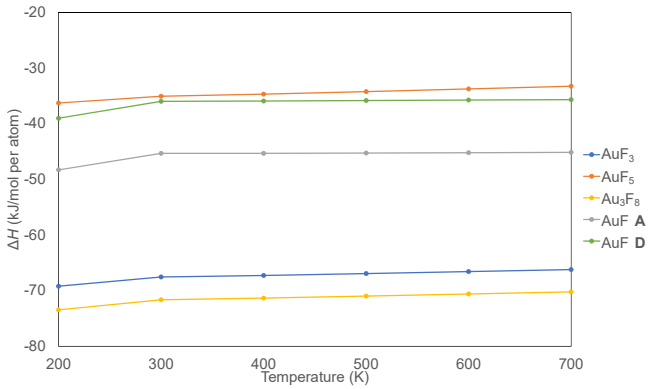

Figure 6. Calculated enthalpy of reaction ΔH per atom for the reaction $x\mathrm{Au} + y\mathrm{F_2} \longrightarrow \mathrm{Au}_x\mathrm{F}_{2y}$ between 200 and 700 K (eq. 2).

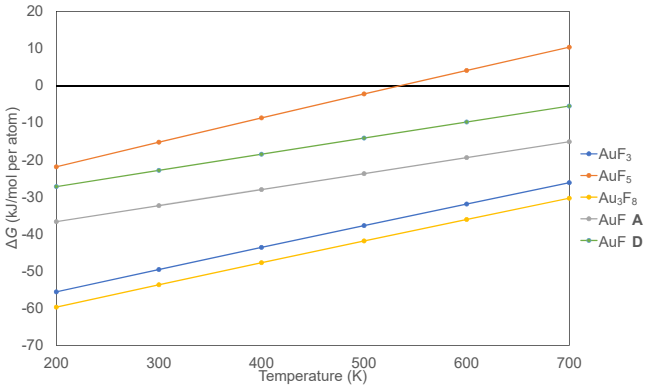

Figure 7. Calculated Gibbs energy of reaction ΔG per atom for the reaction $x\mathrm{Au} + y\mathrm{F_2} \longrightarrow \mathrm{Au}_x\mathrm{F}_{2y}$ between 200 and 700 K (eq. 2).

formation of Au(I)F is not energetically favorable. This is further supported by our extensive study on the energetics and thermodynamics of the hypothetical AuF crystal structures. The formation of Au(I)F is not favored over the mixed-valence $Au_3[AuF_4]$ species even at pressures as high as 25 GPa, making the synthesis, isolation, and characterisation of Au(I)F a very demanding task. Nevertheless, our systematic investigation provides a broad overview on the thermodynamic stability of aurophilic binary gold fluorides at different pressures and temperatures and suggests the existence of interesting mixed-valence "AuF" species $Au_3[AuF_4]$.

ACKNOWLEDGMENTS

We thank Dr. Sergei Ivlev (Philipps-Universität Marburg) for very helpful discussions on binary gold fluorides. The work has been funded by the Academy of Finland (grant no. 317273). Computational resources were pro-

vided by CSC, the Finnish IT Center for Science.

[1] A. F. Holleman, E. Wiberg, and N. Wiberg, *Lehrbuch der anorganischen Chemie*, 102nd ed. (de Gruyter, Berlin, 2007) pp. 1433–1482.

[2] B. G. Müller, Fluorides of copper, silver, gold, and palladium, Angew. Chem. Int. Ed. Engl. **26**, 1081 (1987).

[3] E. Janssen, J. Folmer, and G. Wiegers, The preparation and crystal structure of gold monochloride, AuCl, J. Less-Common Met. **38**, 71 (1974).

[4] E. Janssen and G. Wiegers, Crystal growth and the crystal structures of two modifications of gold monobromide, I-AuBr and P-AuBr, J. Less-Common Met. **57**, 47 (1978).

[5] H. Jagodzinski, Die Kristallstruktur des AuJ, Z. Kristallogr. **112**, 80 (1959).

[6] A. G. Sharpe, Auric fluoride and related compounds, J. Chem. Soc. , 2901 (1949).

[7] I. C. Tornieporth-Oetting and T. M. Klapötke, Laboratory scale direct synthesis of pure AuF_3, Chem. Ber. **128**, 957 (1995).

[8] F. W. B. Einstein, P. R. Rao, J. Trotter, and N. Bartlett, The crystal structure of gold trifluoride, J. Chem. Soc. A , 478 (1967).

[9] J. H. Holloway and G. J. Schrobilgen, Krypton fluoride chemistry; a route to AuF_5, $KrF^+AuF_6^-$, $Xe_2F_3^+AuF_6^-$, and $NO^+AuF_6^-$: the KrF^+–$XeOF_4$ system, J. Chem. Soc., Chem. Commun. , 623 (1975).

[10] M. J. Vasile, T. J. Richardson, F. A. Stevie, and W. E. Falconer, Preparation and characterization of gold pentafluoride, J. Chem. Soc., Dalton Trans. , 351 (1976).

[11] I.-C. Hwang and K. Seppelt, Gold pentafluoride: Structure and fluoride ion affinity, Angew. Chem. Int. Ed. **40**, 3690 (2001).

[12] R. E. Stene, B. Scheibe, C. Pietzonka, A. J. Karttunen, W. Petry, and F. Kraus, MoF_5 revisited. A comprehensive study of MoF_5, J. Fluor. Chem. **211**, 171 (2018).

[13] J. Beck and F. Wolf, Three new polymorphic forms of molybdenum pentachloride, Acta Crystallogr. B **53**, 895 (1997).

[14] W. Hönle, S. Furuseth, and H. G. von Schnering, Synthesis and crystal structure of ordered, orthorhombic α-$NbBr_5$, Z. Naturforsch. B **45**, 952 (1990).

[15] S. H. Elder, G. M. Lucier, F. J. Hollander, and N. Bartlett, Synthesis of Au(II) fluoro complexes and their structural and magnetic properties, J. Am. Chem. Soc. **119**, 1020 (1997).

[16] R. Schmidt and B. G. Müller, Einkristalluntersuchungen an $Au[AuF_4]_2$ und CeF_4, zwei unerwarteten Nebenprodukten, Z. Anorg. Allg. Chem. **625**, 605 (1999).

[17] A. A. Timakov, V. N. Prusakov, and Y. V. Drobyshevskii, Gold heptafluoride, Dokl. Akad. Nauk SSSR **291**, 125 (1986).

[18] S. Riedel and M. Kaupp, Has AuF_7 been made?, Inorg. Chem. **45**, 1228 (2006).

[19] D. Himmel and S. Riedel, After 20 years, theoretical evidence that "AuF_7" is actually $AuF_5{\cdot}F_2$, Inorg. Chem. **46**, 5338 (2007).

[20] S. S. Nabiev, V. B. Sokolov, S. N. Spirin, and B. B. Chaivanov, Synthesis and spectral properties of hexafluoroaurates, Russ. J. Phys. Chem. A **85**, 1931 (2011).

[21] T. Waddington, The lattice energies and thermodynamic properties of the hypothetical compounds AuF and CuF, Trans. Faraday Soc. **55**, 1531 (1959).

[22] P. Schwerdtfeger, M. Dolg, W. H. E. Schwarz, G. A. Bowmaker, and P. D. W. Boyd, Relativistic effects in gold chemistry. I. Diatomic gold compounds, J. Chem. Phys. **91**, 1762 (1989).

[23] P. Schwerdtfeger, J. S. McFeaters, R. L. Stephens, M. J. Liddell, M. Dolg, and B. A. Hess, Can AuF be synthesized? A theoretical study using relativistic configuration interaction and plasma modeling techniques, Chem. Phys. Lett. **218**, 362 (1994).

[24] P. Schwerdtfeger, J. S. McFeaters, M. J. Liddell, J. Hrušák, and H. Schwarz, Spectroscopic properties for the ground states of AuF, AuF^+, AuF_2, and Au_2F_2: A pseudopotential scalar relativistic Møller–Plesset and coupled-cluster study, J. Chem. Phys. **103**, 245 (1995).

[25] D. Schröder, J. Hrušák, I. C. Tornieporth-Oetting, T. M. Klapötke, and H. Schwarz, Neutral gold(I) fluoride does indeed exist, Angew. Chem. Int. Ed. Engl. **33**, 212 (1994).

[26] S. Andreev and J. J. BelBruno, Detection of AuF by emission spectroscopy in a hollow cathode discharge, Chem. Phys. Lett. **329**, 490 (2000).

[27] C. J. Evans and M. C. L. Gerry, Confirmation of the existence of gold(I) fluoride, AuF: Microwave spectrum and structure, J. Am. Chem. Soc. **122**, 1560 (2000).

[28] X. Wang, L. Andrews, F. Brosi, and S. Riedel, Matrix infrared spectroscopy and quantum-chemical calculations for the coinage-metal fluorides: Comparisons of Ar–AuF, Ne–AuF, and molecules MF_2 and MF_3, Chem.: Eur. J. **19**, 1397 (2013).

[29] T. Söhnel, H. Hermann, and P. Schwerdtfeger, Towards the understanding of solid-state structures: From cubic to chainlike arrangements in group 11 halides, Angew. Chem. Int. Ed. **40**, 4381 (2001).

[30] T. Söhnel, H. Hermann, and P. Schwerdtfeger, Solid state density functional calculations for the group 11 monohalides, J. Phys. Chem. B **109**, 526 (2005).

[31] D. Kurzydłowski and W. Grochala, Elusive AuF in the solid state as accessed via high pressure comproportionation, Chem. Commun. **9**, 1073 (2008).

[32] D. Kurzydłowski and W. Grochala, Xenon as a mediator of chemical reactions? Case of elusive gold monofluoride, AuF, and its adduct with xenon, XeAuF, Z. Anorg. Allg. Chem. **634**, 1082 (2008).

[33] E. Zurek and W. Grochala, Predicting crystal structures and properties of matter under extreme conditions via quantum mechanics: the pressure is on, Phys. Chem. Chem. Phys. **17**, 2917 (2015).

[34] A. R. Oganov, C. J. Pickard, Q. Zhu, and R. J. Needs, Structure prediction drives materials discovery, Nat. Rev. Mater. **4**, 331–348 (2019).

[35] D. M. Deaven and K. M. Ho, Molecular geometry optimization with a genetic algorithm, Phys. Rev. Lett. **75**, 288 (1995).

[36] S. M. Woodley, P. D. Battle, J. D. Gale, and C. Richard A. Catlow, The prediction of inorganic crystal structures

using a genetic algorithm and energy minimisation, Phys. Chem. Chem. Phys. **1**, 2535 (1999).
[37] A. R. Oganov and C. W. Glass, Crystal structure prediction using ab initio evolutionary techniques: Principles and applications, J. Chem. Phys. **124**, 244704 (2006).
[38] A. Hermann, M. Derzsi, W. Grochala, and R. Hoffmann, AuO: Evolving from dis- to comproportionation and back again, Inorg. Chem. **55**, 1278 (2016).
[39] A. G. Kvashnin, A. R. Oganov, A. I. Samtsevich, and Z. Allahyari, Computational search for novel hard chromium-based materials, J. Phys. Chem. Lett. **8**, 755 (2017).
[40] X. Yu, A. R. Oganov, Q. Zhu, F. Qi, and G. Qian, The stability and unexpected chemistry of oxide clusters, Phys. Chem. Chem. Phys. **20**, 30437 (2018).
[41] M. S. Kuklin and A. J. Karttunen, Crystal structure prediction of magnetic transition-metal oxides by using evolutionary algorithm and hybrid DFT methods, J. Phys. Chem. C **122**, 24949 (2018).
[42] M. S. Kuklin, L. Maschio, D. Usvyat, F. Kraus, and A. J. Karttunen, Evolutionary algorithm-based crystal structure prediction for copper(I) fluoride, Chem.: Eur. J. **25**, 11528.
[43] G. Liu, X. Feng, L. Wang, S. A. T. Redfern, Y. Xue, G. Gao, and H. Liu, Theoretical investigation of the valence states in Au via the Au-F compounds under high pressure, Phys. Chem. Chem. Phys. **21**, 17621 (2019).
[44] A. R. Oganov, A. O. Lyakhov, and M. Valle, How evolutionary crystal structure prediction works—and why, Acc. Chem. Res. **44**, 227 (2011).
[45] A. O. Lyakhov, A. R. Oganov, H. T. Stokes, and Q. Zhu, New developments in evolutionary structure prediction algorithm USPEX, Comput. Phys. Commun. **184**, 1172 (2013).
[46] C. W. Glass, A. R. Oganov, and N. Hansen, USPEX—evolutionary crystal structure prediction, Comput. Phys. Commun. **175**, 713 (2006).
[47] R. Dovesi, A. Erba, R. Orlando, C. M. Zicovich-Wilson, B. Civalleri, L. Maschio, M. Rérat, S. Casassa, J. Baima, S. Salustro, and B. Kirtman, Quantum-mechanical condensed matter simulations with crystal, Wiley Interdiscip. Rev. Comput. Mol. Sci. **8**, e1360 (2018).
[48] J. P. Perdew, K. Burke, and M. Ernzerhof, Generalized gradient approximation made simple, Phys. Rev. Lett. **77**, 3865 (1996).
[49] C. Adamo and V. Barone, Toward reliable density functional methods without adjustable parameters: The PBE0 model, J. Chem. Phys. **110**, 6158 (1999).
[50] P. Pyykkö, Strong closed-shell interactions in inorganic chemistry, Chem. Rev. **97**, 597 (1997).
[51] P. Pyykkö, Theoretical chemistry of gold, Angew. Chem. Int. Ed. **43**, 4412 (2004).
[52] H. Schmidbaur and A. Schier, Aurophilic interactions as a subject of current research: An up-date, Chem. Soc. Rev. **41**, 370 (2012).
[53] S. Grimme, J. Antony, S. Ehrlich, and H. Krieg, A consistent and accurate ab initio parametrization of density functional dispersion correction (DFT-D) for the 94 elements H-Pu, J. Chem. Phys. **132**, 154104 (2010).
[54] S. Grimme, A. Hansen, J. G. Brandenburg, and C. Bannwarth, Dispersion-corrected mean-field electronic structure methods, Chem. Rev. **116**, 5105 (2016).
[55] R. E. Stene, B. Scheibe, C. Pietzonka, A. J. Karttunen, W. Petry, and F. Kraus, Mof5 revisited. a comprehensive study of mof5, Journal of Fluorine Chemistry **211**, 171 (2018).
[56] S. I. Ivlev, A. V. Malin, A. J. Karttunen, R. V. Ostvald, and F. Kraus, Reactions of kbrf4 with platinum metals, Journal of Fluorine Chemistry **218**, 11 (2019).
[57] F. Weigend and R. Ahlrichs, Balanced basis sets of split valence, triple zeta valence and quadruple zeta valence quality for H to Rn: Design and assessment of accuracy, Phys. Chem. Chem. Phys. **7**, 3297 (2005).
[58] F. Pascale, C. M. Zicovich-Wilson, F. López Gejo, B. Civalleri, R. Orlando, and R. Dovesi, The calculation of the vibrational frequencies of crystalline compounds and its implementation in the CRYSTAL code, J. Comput. Chem. **25**, 888 (2004).
[59] C. M. Zicovich-Wilson, F. Pascale, C. Roetti, V. R. Saunders, R. Orlando, and R. Dovesi, Calculation of the vibration frequencies of α-quartz: The effect of Hamiltonian and basis set, J. Comput. Chem. **25**, 1873 (2004).
[60] U. Engelmann and B. G. Müller, Darstellung und Struktur der Tetrafluoroaurate(III) $M^I[AuF_4]$ mit M^I = Li, Rb, Z. Anorg. Allg. Chem **598**, 103 (1991).
[61] R. Hoppe and R. Homann, Neue Untersuchungen an Fluorkomplexen mit dreiwertigem Silber und Gold, Z. Anorg. Allg. Chem **379**, 193 (1970).
[62] R. Schmidt and B. G. Müller, Einkristalluntersuchungen an $Cs[AuF_4]$, $Cs[Au_2F_7]$ und $U_2F_7[AuF_4]$, Z. Anorg. Allg. Chem **630**, 2393 (2004).
[63] E. R. Jette and F. Foote, Precision determination of lattice constants, J. Chem. Phys. **3**, 605 (1935).
[64] A. Williams, Neutron powder diffraction study of silver subfluoride, J. Phys. Condens. Matter **1**, 2569 (1989).
[65] N. Hamada, S. Ido, K. Kitazawa, and S. Tanaka, Band structure of Ag_2F, J. Phys. C: Solid State Phys. **19**, 1355 (1986).
[66] S. Ido, S. Uchida, K. Kitazawa, and S. Tanaka, Galvanomagnetic properties and anisotropy of Ag_2F, J. Phys. Soc. Jpn. **57**, 997 (1988).
[67] A. V. Krukau, O. A. Vydrov, A. F. Izmaylov, and G. E. Scuseria, Influence of the exchange screening parameter on the performance of screened hybrid functionals, J. Chem. Phys. **125**, 224106 (2006).
[68] A. Walsh, R. Catlow, R. Galvelis, D. Scanlon, F. Schiffmann, A. A. Sokol, and S. Woodley, Prediction on the existence and chemical stability of cuprous fluoride, Chem. Sci. **3**, 2565 (2012).
[69] A. A. Woolf, The heat of formation of auric and thallic fluorides., J. Chem. Soc. , 4694 (1954).
[70] O. Kubaschewski and O. von Goldbeck, The thermochemistry of gold, Gold Bull. **8**, 80 (1975).
[71] A. F. Vorobiev, L. P. Voloshko, V. A. Legasov, and V. B. Sokolov, The enthalpies of formation of gold pentafluoride and gold trifluoride, Dokl. Akad. Nauk SSSR **286**, 653 (1986).
[72] D. Himmel and S. Riedel, After 20 years, theoretical evidence that "AuF_7" is actually $AuF_5 \cdot F_2$, Inorg. Chem. **46**, 5338 (2007).